

## Research Article

# A Multiobjective Optimization Analysis of Spur Gear Pair: The Profile Shift Factor Effect on Structure Design and Efficiency

Samya Belarhzal <sup>1</sup>, Kaoutar Daoudi,<sup>1</sup> El Mostapha Boudi,<sup>1</sup> Aziz Bachir,<sup>1</sup>  
and Samira Elmoumen<sup>2</sup>

<sup>1</sup>Mechanical Department, Mohammadia School of Engineers, Mohammed V University, Rabat, Morocco

<sup>2</sup>LIMSAD, Fsc, Hassan II University of Casablanca, Casablanca, Morocco

Correspondence should be addressed to Samya Belarhzal; [belarhzal.samya.1@gmail.com](mailto:belarhzal.samya.1@gmail.com)

Received 20 September 2020; Revised 12 January 2021; Accepted 15 January 2021; Published 28 January 2021

Academic Editor: José António Fonseca de Oliveira Correia

Copyright © 2021 Samya Belarhzal et al. This is an open access article distributed under the Creative Commons Attribution License, which permits unrestricted use, distribution, and reproduction in any medium, provided the original work is properly cited.

Spur gears are an indispensable element of power transmission, most of the time used in small environments with severe operating conditions such as high temperature, vibrations, and humidity. For this reason, manufacturers and transmission designers are required to look for better gear designs and higher efficiency. In this paper, a multiobjective optimization was conducted, using genetic algorithms (GAs) for corrected spur gear pair with an objective to reduce the structure volume and transmission power loss and reveal the influence of the profile shift factor on the optimal structure fitness. The optimization variables included are the pinion and wheel profile shift factors in addition to the module, face width, and the number of pinion teeth mostly used in standard gear optimization. The profile shift factor influences the shape of the gear teeth, the contact ratio, and the load sharing. It affects then the optimal results meaningfully. The gear pair volume, center distance, and efficiency presented the objective functions while contact stress, bending stress, face with coefficient, and tooth tip interferences served as constraints. Furthermore, a volume equation was developed, in which a bottom clearance formula is included for more accurate results. "Multiobjective optimization" is conducted at medium and high speeds, and the results show that the structure design is compact compared to standard gears with reasonable efficiency for medium contact ratio.

## 1. Introduction

Gears are used in the industrial field for motion transmission from one shaft to another. They can work in small sizes like those mounted in watches or can be robust and heavy in powerful machines [1]. Gears can also operate under severe conditions, such as resisting pitting and bending stress, power losses, and other environmental issues [2]. Nowadays, transmission designers look forward to obtain optimal structure designs in order to guarantee the system's efficiency and safety and to satisfy economic requirements, as well as handling the effect of operating constraints.

Researchers were first interested in reducing gear size and weight. Yokota et al. [3] were among the first to use genetic algorithms in weight/volume gear optimization. They analyzed the efficiency of an improved program using

nonlinear constraints and integer programming (NIP), reducing the structure's volume by 33.6%.

Thompson et al. [4] then presented a global, multi-optimization design of two- and three-stage spur gears combining double objective functions. The approach shows the relationship between the pitting effect and minimum structure volume. It was proved that the approach is valid and its findings may help for future gear design development. In order to obtain a minimum volume, Gologlu and Zeyveli [5] proposed an automating initial model of gears using dynamic and static functions as penalty functions that improved the results of the GA approach. The optimum structure variables generated the number of teeth, module, and face width. For more accurate results in volume optimization, Wang et al. [6] treated on the volume structure of a transmission single-stage spur gear system. He analyzed the effect of bottom clearance and

addendum factor on optimization results, discussing different structures of spur gears.

In addition to volume and weight [7], efficiency has been the subject of many optimizations analyses using GAs. Gear transmission efficiency is related to the heat generated while gearing, due to either friction in the system or oil churning; this could be the reason for several gear failures, such as scoring or contact fatigue failures. More efficient gears would generate less heat, thus reducing the charge of fuel needed [8].

Petry-Johnson's approach [9] analyzed the efficiency results of spur gears under high speed and torque. At this level, gear mesh efficiency is relatively constant while the total efficiency is not. The same author showed that the surface quality and gear module have the greatest influence on the gear mesh efficiency for high values of speed and torque. Patil et al. [10] analyzed the effect of tribological constraints (scuffing and wear) on volume and efficiency minimization for a two-stage helical gearbox. The multi-optimization with tribological constraints led to less power loss and to the very rare possibility of system failure. In conclusion, volume and efficiency are both crucial to transmission system designers. That leads to the need for combining the structure design and efficiency in one multi-optimization analysis using genetic algorithms.

When it comes to the profile shift factor, Gebremariam et al. [11] assumed that an increase of this factor changed the load sharing properties of a spur gear pair and the system efficiency [12]. Diez-Ibarbia et al. [13] developed three different models of spur gears to visualize the effect of the shifting profile on efficiency under different operating conditions. The authors concluded that the higher the torque and profile shift, the lower the efficiency. Also, the higher the spin speed, the greater the efficiency. It should be noted that they considered the geometry of corrected gears with the same center distance as much as the standard gear pair geometry ( $x_1 + x_2 = 0$ ).

Miler et al. [14] further found that the profile shift factor for pinion and gear is an optimization variable, in addition to the module, the number of pinion teeth, and face width. The addendum diameter was placed on the volume equation, rather than the pitch diameter, to highlight the impact of the shift coefficient on the objective function. After analyzing three sets of data, the gear pair weight was reduced by 32.3% to 34.7%.

This paper presents an extension of previous research studies in the field. The objective of the authors was to obtain the optimum design of a spur gear reducer giving the transmission designers the chance to select the best parameter values. This paper presents an extension of previous researches in the field. The objective of the authors was to obtain the optimum design of a spur gear reducer and then give the transmission designers the chance to select the best parameter values to reach the minimum structure volume, center distance, and power loss. The main novelty of this study was including the bottom clearance volume equation for greater accuracy and increasing the effect of the profile shift factor on volume optimization. The pinion and gear profile shift factors were considered as function variables in the corrected gear model in addition to the module, the teeth face width, and pinion number of teeth, previously used in the standard gear model. The wheel number of teeth was calculated using the transmission factor  $i$ . For more precision, the

multiobjective optimization results for corrected and standard spur gears were compared using genetic algorithms.

## 2. Method

The authors of this paper compare two models of multi-objective optimization using GAs combined with ISO Standard 6336:2006 adopted for the computation of gear load capacity. The structure analyzed is a solid structure pair, as shown in Figure 1. For the first model, three variables are chosen: module  $m$ , face width  $b$ , and the number of teeth on pinion  $Z_1$ . The pinion and wheel profile shift factor  $x_1$  and  $x_2$  are added as variables in the second model of spur gear reducer optimization to study their effect on structure volume, efficiency, and center distance as objective functions. The optimization process is described by the flowchart in Figure 2 and summarized by using the data in Table 1.

*2.1. Genetic Algorithm.* The objective was to reduce the volume structure and center distance while improving system efficiency. For this reason, a multiobjective optimization was considered using the gamultiobj function with a genetic algorithm toolbox of Matlab software [15]. The three objective functions are as follows:

- (1)  $F_1(b, m, Z_1, x_1, x_2)$ : volume minimization
- (2)  $F_2(m, Z_1)$ : center distance minimization
- (3)  $F_3(\eta)$ : efficiency maximization

The process for two considered models (with and without a profile shift factor) is conducted using torque  $T$ , which is the sum of input torque  $T_1$  and the starting torque created by the gear pair moment of inertia at the beginning of the operation:

$$T = T_1 + \frac{\pi^2 n p}{16 t_{st}} m^4 Z_1^4 b (1 + i^2). \quad (1)$$

The different algorithm variables are limited using boundary conditions in order to obtain feasible solutions as indicated in Table 2. The wheel number of teeth  $Z_2$  is calculated using power transmission  $i$ .

In optimization algorithms, the size of the population has a significant influence on the computation time and the accuracy of the results. Raising the initial population size increases the number of generations leading to solution convergence [16]. For this multi-optimization analysis, the population size used was 500 individuals considered as random vectors for initial population variables. The algorithm was generated more than five times for each model for more accurate calculations.

In order to restrict the domain of definition, the algorithm contains several constraint functions, implementing all limits and developing feasible solutions in real situations [17]. The constraint functions are given as follows:

- (1) Contact and bending stress are the most common reasons for material deterioration and system failure [18]. Based on ISO Standard 6336:2006, contact and bending stress constraints are formulated as follows:

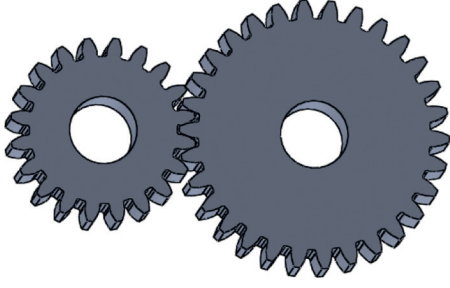


FIGURE 1: Spur gear pair solid structure.

$$g_1(x) = Z_H Z_E Z_\epsilon Z_\beta \sqrt{\frac{W_t}{b \cdot d} \frac{i+1}{i} K_A K_v K_{H\beta} K_{H\alpha}} - \sigma_{Hlim}, \quad (2)$$

$$\sigma_H = \frac{F_t}{b \cdot m} Z_F Z_S Z_\epsilon Z_\beta - \sigma_{Flim}, \quad (3)$$

where the contact stress safety factor  $S_H$  and bending stress safety factor  $S_F$  were taken into consideration (Table 1):

$$\sigma_H = \frac{\sigma_{Hlim}}{S_{Hmin}}, \quad (4)$$

$$\sigma_F = \frac{\sigma_{Flim}}{S_{Fmin}}.$$

- (2) In practical situations, a contact ratio superior to 1.2 is recommended, as it is generally reduced due to mounting inaccuracies. Plus, it can lead to more system vibration and noise. For this reason, another function constraint is added to the algorithm:

$$g_3(x) = \epsilon_\alpha - 1.2. \quad (5)$$

- (3) The face width coefficient  $k = b \cdot m$  should be higher than six and lower than twelve ( $6 < k < 12$ ), which leads to the following two constraints:

$$g_4(x) = 6 - \frac{b}{m}, \quad (6)$$

$$g_5(x) = \frac{b}{m} - 12. \quad (7)$$

- (4) Varying the profile shift factor changes the shape of the gear teeth and influences the center distance modification. This variation could increase the contact ratio value and provoke tooth tip interference [19]. To prevent this undesirable occurrence, the constraint functions (8) and (9) are considered:

$$g_6(x) = \frac{17 - Z_1}{17} - x_1, \quad (8)$$

$$g_7(x) = \frac{17 - Z_2}{17} - x_2. \quad (9)$$

**2.2. Volume and Center Distance Calculation.** The model volume structure for spur gears analyzed in this paper is a

solid structure pair, as shown in Figure 1. The wheel and pinion are considered as two cylinders. In this case, the gear pitch diameter  $d$  is cylinder diameter ( $d = m \cdot Z$ ), and the height is assumed as the teeth width  $b$ . The structure equation volume for standard spur gear pair is written as follows:

$$V = f(m, b, Z_1) = V_w + V_p = \frac{\pi b m^2 Z_1^2 (1 + i^2)}{4}, \quad (10)$$

in which  $m$  is the module,  $Z_1$  is the pinion number of teeth, and  $i$  is the transmission factor ( $Z_2 = i \cdot Z_1$ ).

The gear volume contains two main parts: the tooth and the spoke. The tooth part is the part between the root diameter and the pitch diameter of the gear. Clearance occurs as the backlash between the root circle of one wheel and the addendum circle of the mating wheel to guarantee smooth gearing [20]. Figure 3 presents the 3D model of the bottom clearance volume.  $S_a$  is the tip thickness of the mating wheel.  $Z_1$  is the number of pinion teeth, and  $b$  the face width of the spur gear pair. The equation of the bottom clearance for the pinion is as follows:

$$V_{c1} = S_{a1} * h_1 * b * Z_1. \quad (11)$$

Varying the profile shift factor  $x$  will directly impact the shape of the spur gear teeth. It changes the values of the addendum, the dedendum, the high clearance  $h$ , and the tip thickness [21]. In this case, the solid structure volume for corrected spur gear pair is a function of module  $m$ , face width  $b$ , pinion number of teeth  $Z_1$ , and the profile shift factor for pinion and gear  $x_1$  and  $x_2$ , respectively (equation (14)):

$$S_{a1} = S * \frac{r_{a1}}{r_1} - 2r_{a1} * (\text{inv}\alpha_{a1} - \text{inv}\alpha),$$

$$S_1 = m * \left( \frac{\pi}{2} + 2x_1 \tan \alpha \right), \quad (12)$$

$$h_1 = (0.25 - 2x_1) * m,$$

$$\alpha_{a1} = \arccos \frac{r_{b1}}{r_{a1}},$$

$$\text{inv}\alpha_{a1} = \tan \alpha_{a1} - \alpha_{a1},$$

$$r_{a1} = m * \left( \frac{Z_1}{2} + x_1 + 1 \right), \quad (13)$$

$$r_1 = m * \frac{Z_1}{2},$$

$$r_{b1} = m * \frac{Z_1}{2} \cos \alpha.$$

$$V' = f(m, b, Z_1, x_1, x_2) = \frac{\pi b m^2 Z_1^2 (1 + i^2)}{4 - V_c}. \quad (14)$$

The center distance  $a$  is the length between the pinion center and the wheel center [22]. The formula of  $a$  is given by

$$a = \frac{m \cdot Z_1}{2} \cdot (1 + i). \quad (15)$$

**2.3. Efficiency Calculation.** Efficiency is the degree of success of systems in reaching the desired results. It is defined as the

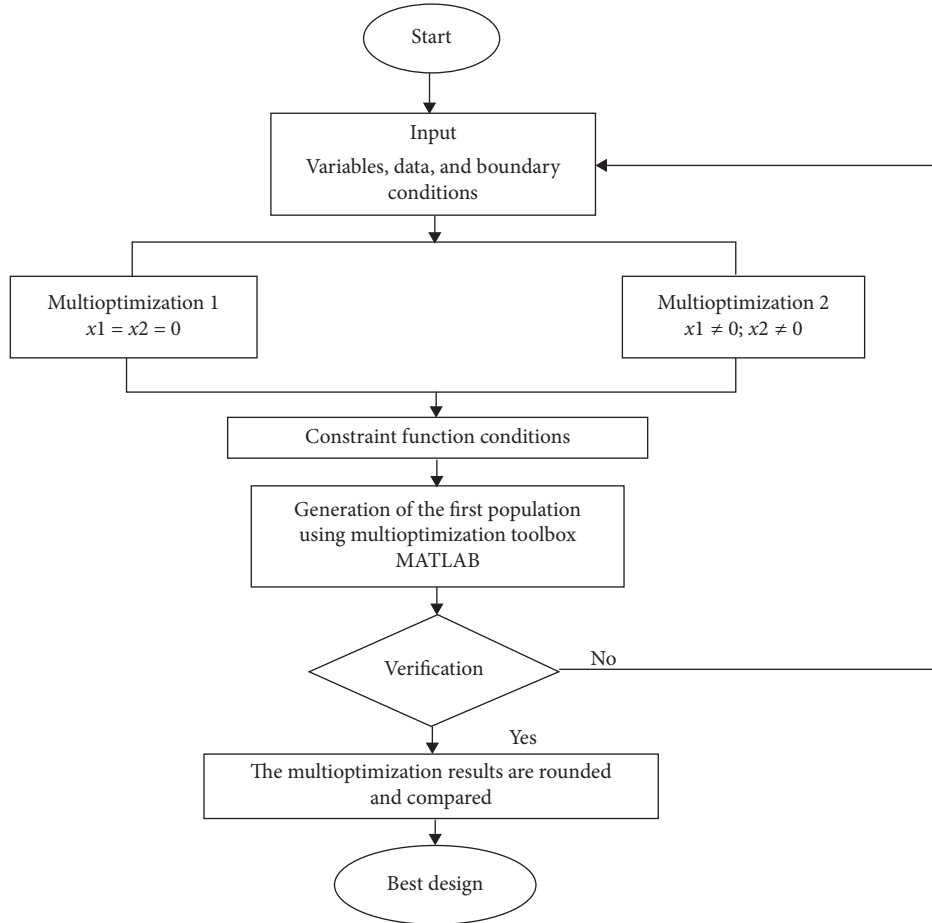


FIGURE 2: Multioptimization process flowchart.

TABLE 1: Multioptimization input data.

Parameter	Value
Pinion shaft diameter (mm)	20
Gear shaft diameter (mm)	20
Input speed (tr/min)	720
Poisson's ratio	0.3
Elasticity factor (GPa)	210
Torque $T_1$ (N·m)	250
Transmission ratio $i$	2.8
Maximum bending stress $\sigma_{F\max}$ (MPa)	750
Maximum contact stress $\sigma_{H\max}$ (MPa)	450
Density $\rho$ [(Kg/m <sup>3</sup> )]	7830
Starting time $t_{st}$ (s)	2
Contact stress safety factor $S_{H\min}$	1.2
Bending stress safety factor $S_{F\min}$	1.2
Material	Standard steel

TABLE 2: Multioptimization boundary conditions.

Input variables	Range
Module $m$ (mm)	(4,10)
Pinion number of teeth $Z_1$	(23,30)
Face width $b$	(6,120)
Pinion profile shift factor $x_1$	(0,0.7)
Wheel profile shift factor $x_2$	(-0.7,0.7)

Based on the Hohn [23] approach, the dependent-load losses depend on gear geometry equation (20) and lubricant properties equation (24). The loss degree formula is as follows:

$$\zeta = \frac{P_{\text{loss}}}{P_{\text{in}}} = 1 - \eta, \quad (16)$$

quotient between the useful and the chosen power. Generally, power loss is either load-dependent such as the loss of power due to the friction between meshing gear teeth, or load-independent, such as oil churning and squeezing. Power loss can also occur from bearing losses and seal power loss [8]. As the independent loads are more dominant in high-speed cases, the authors of this paper only considered dependent-load power loss resulting from frictional effects [13].

where  $P_{\text{loss}}$  is the entire power loss resulting from the heat generated between the spur gear pair teeth in contact while meshing,  $P_{\text{in}}$  is the input power used, and  $\eta$  is the degree of efficiency. The final equation of the power loss rests on two main assumptions: the constant friction coefficient over the path of contact, and the load sharing analytically explained by the literature from Standard ISO/TC-60 [24]. The approach is explained in detail in [23], and [25]. The power loss and efficiency equations are as follows:

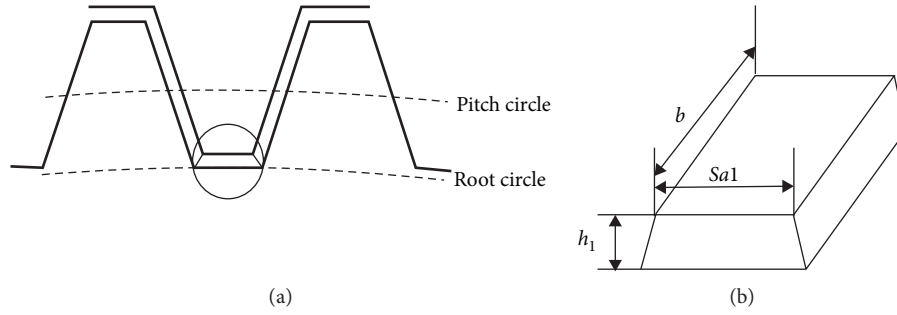


FIGURE 3: The bottom clearance model calculation.

$$P_{\text{loss}} = P_{\text{in}} \mu_m H_v, \quad (17)$$

$$\eta = \frac{P_{\text{out}}}{P_{\text{in}}} = \frac{P_{\text{in}} - P_{\text{loss}}}{P_{\text{in}}} = \frac{P_{\text{in}} - P_{\text{in}} \mu_m H_v}{P_{\text{in}}}, \quad (18)$$

$$\eta = 1 - \mu_m H_v, \quad (19)$$

where  $H_v$  is the power loss factor and  $\mu_m$  is the coefficient of friction. It is clear from (17) and (20) that the power loss depends on the structure's geometry conditions presented by  $H_v$ . It is defined according to the number of pinion teeth  $Z_1$ , transmission ratio  $i$ , contact ratio  $\varepsilon_\alpha$ , and the addendum contact ratio for pinion  $\varepsilon_1$  and gear  $\varepsilon_2$ . For spur gears  $\cos \beta = 1$ ,

$$H_v = \frac{\pi}{Z_1 \cos \beta} \cdot \frac{1+i}{i} \cdot (1 - \varepsilon_\alpha + \varepsilon_1^2 + \varepsilon_2^2), \quad (20)$$

where  $\varepsilon_\alpha$  is the average number of gear pairs in contact simultaneously [11]. It is also presented as the length of the contact line  $\overline{AB}$  divided by the base pitch  $p_b$  [26] (Figure 4). The value of  $\varepsilon_\alpha$  depends mainly on the shape of the spur gear teeth for the pinion and wheel [27]. For corrected gears (nonstandard), the teeth parameters are influenced by the profile shift factor value  $x$ , such as the tooth thickness  $S$  (12), bottom clearance  $h$ , and the addendum and dedendum values. As shown in Figure 5, the contact ratio increases by augmenting the profile shift factor for both pinion and wheel:

$$\varepsilon_\alpha = \frac{\overline{AB}}{p_b} = \varepsilon_1 + \varepsilon_2, \quad (21)$$

$$\varepsilon_1 = (1 + x_1) \cdot \frac{1}{\pi \cdot \cos \alpha} \cdot \left( \sqrt{\left( \frac{Z_1}{2(1+x_1)} \cdot \sin \alpha \right)^2 + \frac{Z_1}{1+x_1} + 1} - \frac{Z_1}{2(1+x_1)} \cdot \sin \alpha \right), \quad (22)$$

$$\varepsilon_2 = (1 + x_2) \cdot \frac{1}{\pi \cdot \cos \alpha} \cdot \left( \sqrt{\left( \frac{Z_1 \cdot i}{2(1+x_2)} \cdot \sin \alpha \right)^2 + \frac{Z_1 \cdot i}{1+x_2} + 1} - \frac{Z_1 \cdot i}{2(1+x_2)} \cdot \sin \alpha \right). \quad (23)$$

The formula of friction coefficient  $\mu_m$  was developed using Coulomb's formulation and modeled by the Niemann formulation [28].  $\mu_m$  was constant along the mesh cycle and presented by the following equation:

$$\mu_m = 0,048 \cdot \left( \frac{F_t / l_{\text{min}}}{v_{\Sigma C} \cdot \rho_{\text{redC}}} \right)^{0,2} \cdot \eta_{\text{oil}}^{-0,05} \cdot R_a^{0,25} \cdot X_L, \quad (24)$$

where

$F_t$  is the circumferential force at base circle (N)

$l_m$  is the face width for spur gears (mm)

$v_{\Sigma C}$  is the sum velocity at operating pitch circle (m/s)

$\rho_{\text{redC}}$  is the reduced radius of curvature at pitch point (mm)

$\eta_{\text{oil}}$  is the dynamic oil viscosity at oil temperature (mPas)

$R_a$  is the arithmetic mean roughness ( $\mu\text{m}$ )

$X_L$  is the lubricant correction factor

### 3. Results

An Intel (R) Core (TM) i5-2430M with 8 GB was used to obtain the computation results. The average time of calculation with 300 generations was almost 2 s and standard spur gear optimization converged quickly.

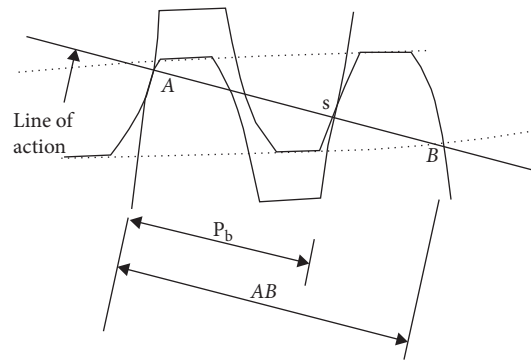


FIGURE 4: The length of contact and the base pitch for meshing spur gear teeth.

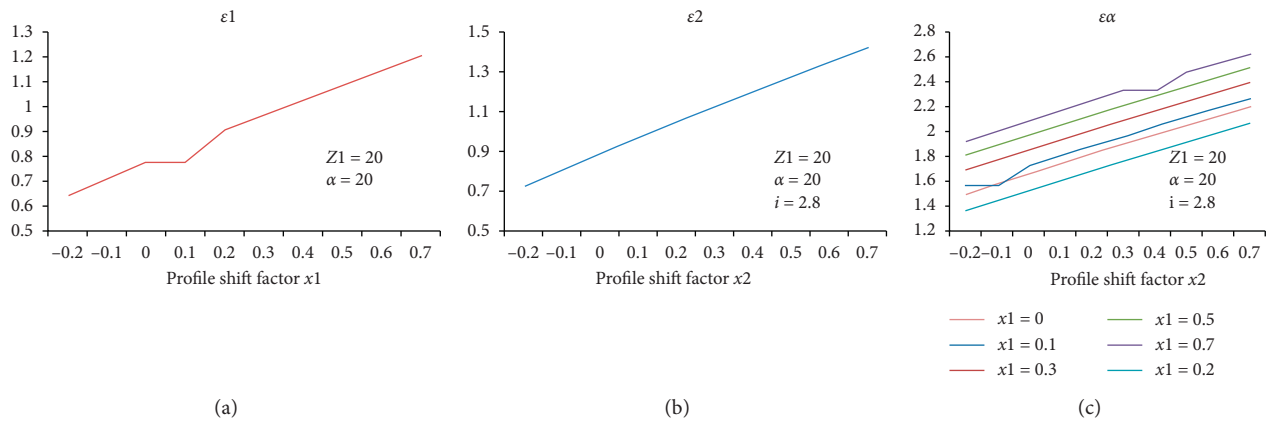


FIGURE 5: Contact ratio plot depending on pinion and wheel shift coefficient.

Tables 3 and 4 present the best fitness values for structure volume, center distance, and efficiency. Optimal design variables for the corrected and standard gears ( $x_1 = x_2 = 0$ ) are provided as well. The multiobjective optimization was performed for normal and high speed, considering the low, medium, and high contact ratio  $\epsilon_\alpha$ . The influence of the profile shift factor was significant in the spur gear pair optimization at normal and high speed. The case with high contact ratio ( $\epsilon_\alpha > 2$ ) gave the minimum volume and center distance for the geometry, 37% and 10% lower than volume and center distance, respectively, for geometry with a medium contact ratio ( $1.6 < \epsilon_\alpha < 2$ ). Similarly, for high  $n$ , the structure volume and center distance were lower for corrected spur gears by 55% and 36%, respectively. The optimization results showed that having a lower volume is reached faster by raising the module and with the pinion profile shift factor  $x_1$  than looking for a compromise between the module and teeth face width.

The Pareto front shown in Figures 6 and 7 presents the best compromise solutions between structure volume and center distance with transmission power loss. For corrected spur gears, a knee zone appears in Figures 6 and 7, which gives the transmission designers a smaller and better set of solutions easy to use in real situations. Around this area, a slight improvement in one objective would lead to a large deterioration in the other objective. In this paper, for

minimum volume values less than  $5.10^6 \text{mm}^3$ , a sharp peak in power loss value provides for corrected spur gears. However, for spur gears without a profile shift factor, the power loss is less for the same volume value. This behavior can be explained by the absence of the knee zone in standard gear Pareto front. The same behavior was observed for center distance and power loss Pareto front.

To make a comparison between solutions of the three objective functions, the 3D Pareto front for optimal solutions is carried out Figure 8. It actually confirms the previous results given by Figures 6 and 7. Always for high values of  $x_1$  and  $x_2$ , the structure design is more compact; however, the power loss is very high compared to standard spur gears.

#### 4. Discussion

The effect of the profile shift factor  $x$  was remarkable in various parameters analyzed in this study. The optimization data showed that the increment of  $x$  and contact ratio  $\epsilon_\alpha$  decreased the profile shift factor  $Z_\epsilon$  by 13% and 4% for normal and high speed, respectively, as  $\epsilon_\alpha$  is inversely dependant to  $\epsilon_\alpha$  (11). As a result of  $Z_\epsilon$  reduction, the contact stress accrued between teeth flank in contact, and bending stress on the root teeth can sharply decrease. The effect of  $x$  on  $Z_\epsilon$  was confirmed by equations (1) and (2) and proved in

TABLE 3: Multioptimization results of the spur gear pair for normal speed.

Multioptimization results	High contact ratio $\varepsilon_\alpha > 2$	$1.6 < \varepsilon_\alpha < 2$	Without profile shift factor
Module $m$	4	4.5	9.5
Face width $b$	36	46	96
Pinion number of teeth $Z_1$	23	24	30
Wheel number of teeth $Z_2$	64	68	84
Pinion profile shift factor $x_1$	0.64	0.2	0
Wheel profile shift factor $x_2$	0.35	0.3	0
Face with coefficient $k$	9	10	10
Volume $V$	2164317.27	3448022.6	59352740.9
Bottom clearance volume $V_{bc}$	14199 (0.66%)	21671 (0.63%)	193560 (0.33%)
Power loss PL	563.85	413.44	164
Efficiency $\eta$	0.974	0.981	0.992
Center distance $a$	176	196.3	569
Contact ratio factor $Z_\varepsilon$	0.566	0.6	0.689

TABLE 4: Multioptimization results of the spur gear pair for high speed.

Multioptimization results	High contact ratio $\varepsilon_\alpha > 2$	$1.6 < \varepsilon_\alpha < 2$	Without profile shift factor
Module $m$	4	5	9.5
Face width $b$	38	47	71
Pinion number of teeth $Z_1$	23	28	29
Wheel number of teeth $Z_2$	64	78	81
Pinion profile shift factor $x_1$	0.44	0.12	0
Wheel profile shift factor $x_2$	0.43	0.05	0
Face with coefficient $k$	9.5	9.4	7.5
Volume $V$	2331408.7	7125068.7	37410501.3
Bottom clearance volume $V_{bc}$	21702 (0.93%)	27327 (0.38%)	120790 (0.32%)
Power loss PL	346.4	157.64	113.6
Efficiency $\eta$	0.984	0.992	0.995
Center distance $a$	178.36	280.57	525.08
Contact ratio factor $Z_\varepsilon$	0.573	0.654	0.682

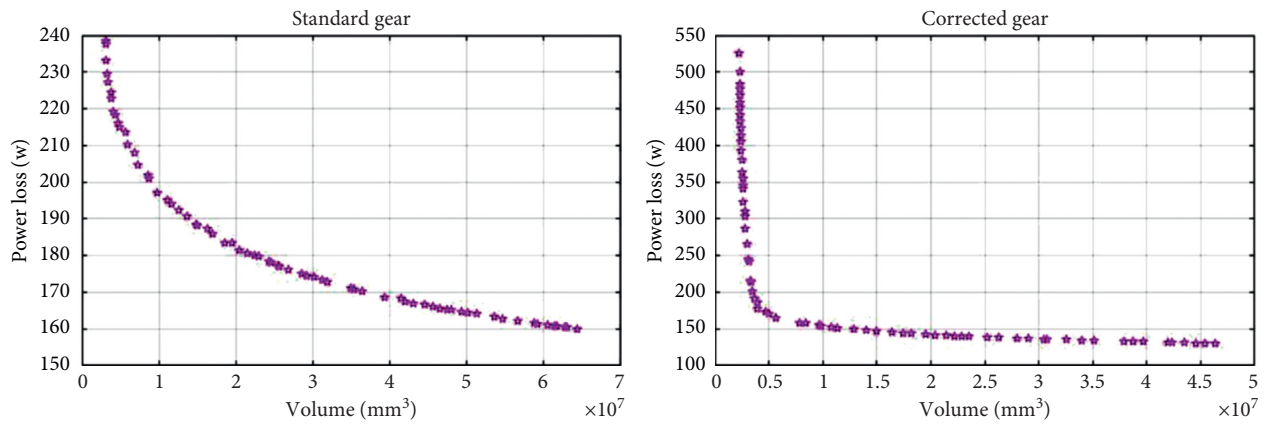


FIGURE 6: Pareto front of GA multioptimization for volume and power loss in case of standard and corrected spur gear pair.

previous studies by the authors using the finite element method [12, 18]:

$$Z_\varepsilon = 0.25 + 0.75CR. \tag{25}$$

In the same context, every time the shift coefficient rises, the bottom clearance  $V_{bc}$  also rises (Table 3 and 4). When using a positive coefficient ( $x > 0$ ), an extended part of the involute is used as a tooth profile. For this

reason, there is a backlash between the tooth profile created when the center distance increases, resulting in the rear flank moving away before touching the flank of the mating gear. The tooth tip gets sharper, which explain the elevation of the space between teeth in contact. Sometimes, it may require shortening a tooth to avoid the undercut phenomenon for corrected gears.

For power loss dependency analysis, only gear elements were taken into account in this paper. Roller bearing and

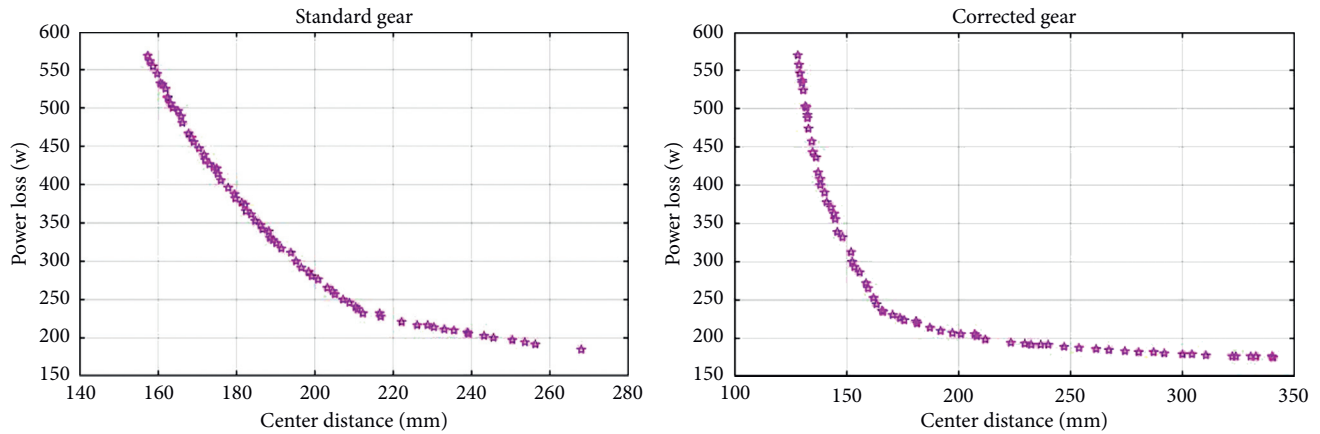


FIGURE 7: Pareto front of GA multioptimization for center distance and power loss in case of standard and corrected spur gear pair.

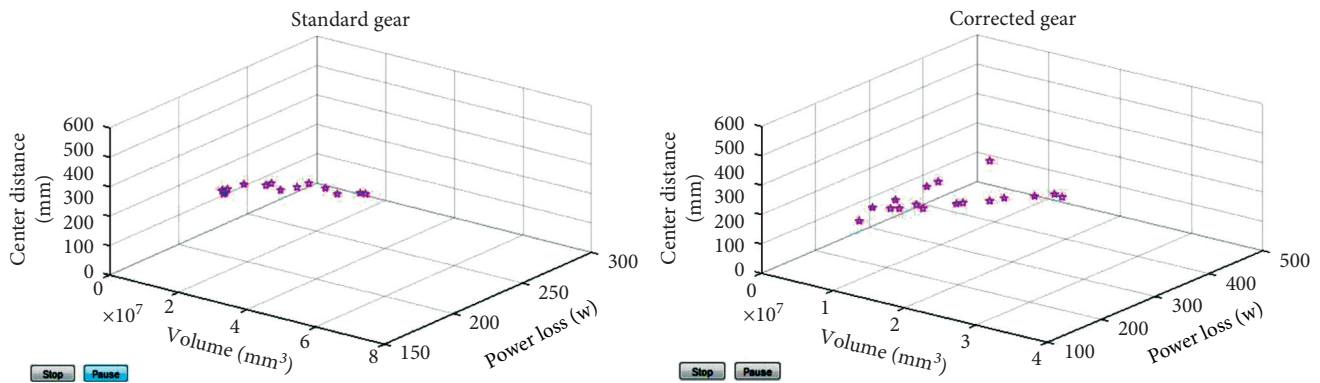


FIGURE 8: 3D Pareto front for volume, power loss, and center distance between corrected and standard spur gear pair.

nondependent load as windage and churning losses were not considered. The highest power loss was 563.85 W ( $\eta = 0.974$ ) corresponding to the lowest volume and center distance Table 3 for corrected spur gears with a high contact ratio ( $CR > 0$ ). At the same time, the results of the optimization revealed that the lower power loss was 164 W ( $\eta = 0.992$ ), corresponding to the maximum volume and center distance for standard gears ( $x_1 = x_2 = 0$ ). In conclusion, reducing the structure volume and center distance to the maximum using high values of  $x$  leads to a significant decrease in system efficiency.  $x_1$  and  $x_2$  have a significant effect on load sharing (LS) distribution. The LS, in turn, greatly impacts the power loss (PL) and, therefore, efficiency, by affecting the power loss factor  $H_v$  [13]. In a previous study [18], the authors found that as much as the pinion and wheel profile shift factor increases, the value of the contact ratio CR increases as well according to equations (22), (23), and (21) and confirmed by multiobjective optimization results presented in Figure 9. The higher the contact ratio, the longer the path of contact. Meaning that when a pair of spur gear teeth are meshing, the start of contact with the next tooth took place sooner than with the lower value of CR. In this case, the LS distribution changes, and the power loss increases.

Figure 10 shows a sharp decrease in system efficiency for high values of pinion and wheel profile shift factor  $x_1$  and  $x_2$ , which confirm the results given by Pareto front in Figures 6 and 7.

Efficiency decreases with the profile shift factor increment as a result of LS variation at the beginning and the end of pair teeth contact as shown in Table 3 and Figure 10.

It was also observed that a rapid change in module value yields an important variation in power loss and efficiency. The results prove that a higher power loss occurs with a lower module  $m$ . This fact could be explained by the elevation of the normal load  $F_N$  on the spur gear teeth while meshing, generated by applying the operating torque  $T_1$ .  $F_N$  is inversely dependent on the module  $m$ . Studies by Naruse [29] and Petry-Johnson [30] found that even power losses resulted from friction increase with module elevation.

Regarding the wheel profile shift factor  $x_2$ , it was the main reason for the power loss increment coupled with a slight increase in volume and center distance. When  $x_2$  increased (positively), it revealed an increase in wheel contact ratio  $\varepsilon_2$  and then contact ratio CR based on equations (21) and (23). This explains the efficiency reduction due to the variation of the load sharing distribution [13]. The slight increment in volume and center distance caused by  $x_2$  corresponds to the increase in the wheel addendum diameter  $d_{a2}$ , as opposed to the wheel size in general.

To better understand the impact of the input speed on the spur gear power loss and efficiency, Figure 11 provides the different graph variations. By increasing the input speed from 750 tr/min to 3000 tr/min, the system power loss is

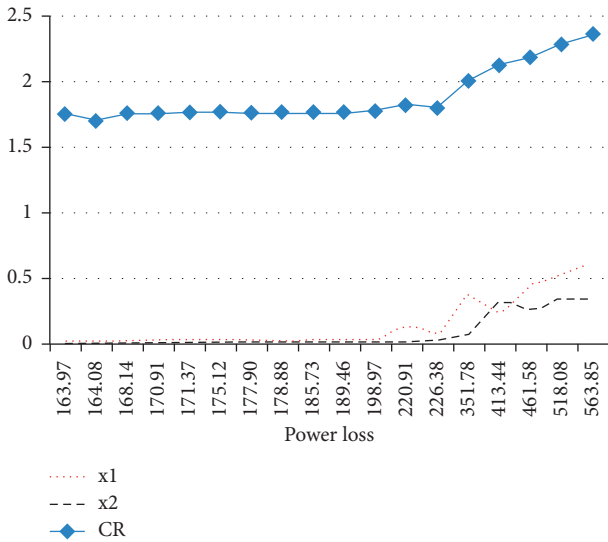


FIGURE 9: Impact of shift coefficient on power loss PL.

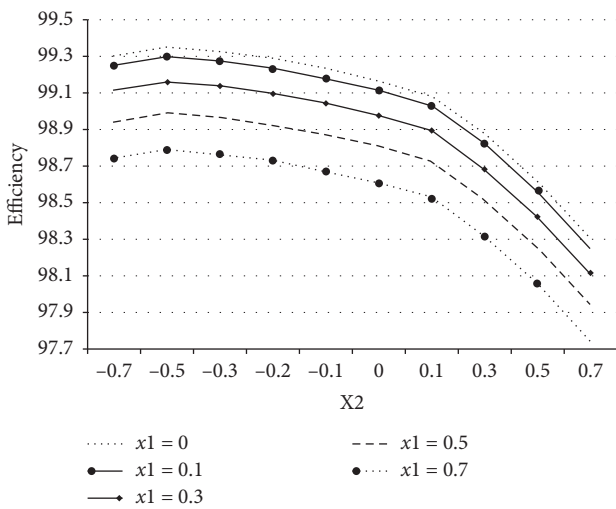


FIGURE 10: Efficiency plots depending on pinion and wheel profile shift factor.

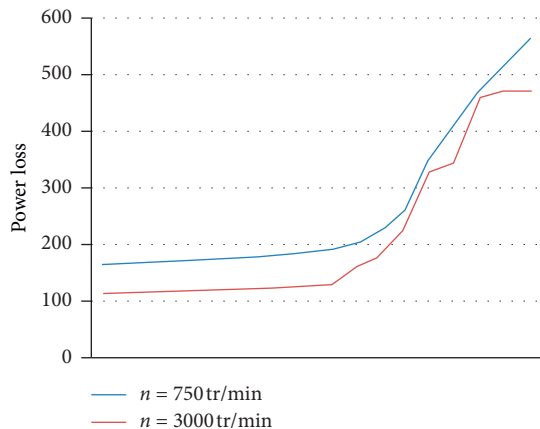


FIGURE 11: Influence of input speed on system power loss PL.

correspondingly increased by 1%, 1.1%, and 0.3% for geometry with high contact ratio ( $CR > 2$ ),  $1.7 < CR < 2$ , and standard spur gear, respectively. The results are shown in Tables 3 and 4.

### 5. Conclusion

This paper sought to realize a multiobjective optimization for one pair of spur gears. Three objective functions were considered: volume, center distance, and efficiency with five parameters as fitness variables: module, teeth face width, pinion number of teeth, pinion profile shift factor, and wheel profile shift factor. For more accuracy, the bottom clearance volume equation was included in the structure volume equation. The optimization results indicate the following:

- (1) With a higher pinion and wheel profile shift factor and  $CR > 2$ , the volume and center distance were reduced by 37% and 10%, respectively.
- (2) Varying the module and the pinion shift coefficient  $x_1$  had more influence on the volume and center distance decrease than did the module and face width.
- (3) The power loss is higher for corrected spur gears, but only with large values of the shift coefficient. Otherwise, the efficiency values are acceptable as much as for standard gears.
- (4) For positive values of  $x_1$ , an increase in the wheel profile shift factor  $x_2$  leads to a reduction in power loss.
- (5) Similarly, the spur gear power loss decreases with an increase in input speed while using a constant input torque.

In conclusion, using a positive and medium shift coefficient, coupled with a large number of teeth and lower face width, leads to a compact design of the pair of spur gears with respect to efficiency, as compared to standard spur gears.

### Data Availability

The data used to support the findings of this study are available from the corresponding author upon request.

### Conflicts of Interest

The authors declare that they have no conflicts of interest.

### References

- [1] G. Zhai, Z. Liang, and Z. Fu, "A mathematical model for parametric tooth profile of spur gears," *Mathematical Problems in Engineering*, vol. 2020, Article ID 7869315, 12 pages, 2020.
- [2] S. Tekeste, *Finite element based surface fatigue estimation in involute spur gear under rolling sliding contact conditions*, Ph.D. thesis, Addis Ababa University, Addis Ababa, Ethiopia, 2011.

- [3] T. Yokota, T. Taguchi, and M. Gen, "A solution method for optimal weight design problem of the gear using genetic algorithms," *Computers and Industrial Engineering*, vol. 35, no. 3, pp. 523–526, 1998.
- [4] D. F. Thompson, S. Gupta, and A. Shukla, "Tradeoff analysis in minimum volume design of multi-stage spur gear reduction units," *Mechanism and Machine Theory*, vol. 35, no. 5, p. 609, 2000.
- [5] C. Gologlu and M. Zeyveli, "A genetic approach to automate preliminary design of gear drives," *Computers and Industrial Engineering*, vol. 57, no. 3, pp. 1043–1051, 2010.
- [6] C. Wang, S. Wang, and G. Wang, "Volume models for different structures of spur gear," *Australian Journal of Mechanical Engineering*, vol. 17, no. 2, pp. 145–153, 2019.
- [7] L. Han, G. Liu, X. Yang, and B. Han, "Dimensional and layout optimization design of multistage gear drives using genetic algorithms," *Mathematical Problems in Engineering*, vol. 2020, Article ID 3197395, 19 pages, 2020.
- [8] B. Clavac and Z.-I. Korka, "Efficiency investigation on a helical gear transmission," *Analele Universității Eftimie Murgu Reșița*, vol. 24, no. 1, 2017.
- [9] T. Petry-Johnson, A. Kahraman, N. Anderson, and D. Chase, "Experimental investigation of spur gear efficiency," in *Proceedings of the ASME 2007 International Design Engineering Technical Conferences & Computers and Information in Engineering Conference*, pp. 747–758, Las Vegas, NV, USA, 2007.
- [10] M. Patil, P. Ramkumar, and K. Shankar, "Multi-objective optimization of the two-stage helical gearbox with tribological constraints," *Mechanism and Machine Theory*, vol. 138, p. 38, 2019.
- [11] M. Gebremariam, A. Thakur, E. Leake, and D. Tilahun, "Effect of change of contact ratio on contact fatigue stress of involute spur gears," *International Journal of Current Engineering and Technology*, vol. 8, no. 3, pp. 719–731, 2018.
- [12] S. Belarhzal, E. M. Boudi, A. BAchir, and Y. Amadane, "Analysis of profile shift factor's effect on bending stress of spur gears using the finite element method," in *Proceedings of the 2020 IEEE 6th International Conference on Optimization and Applications (ICOA)*, pp. 1–6, Mellal, Morocco, April 2020.
- [13] A. Diez-Ibarbia, A. F. del Rincon, M. Iglesias, A. de-Juan, P. Garcia, and F. Viadero, "Efficiency analysis of spur gears with a shifting profile," *Meccanica*, vol. 51, no. 3, pp. 707–723, 2016.
- [14] D. Miler, A. Lončar, D. Žeželj, and Z. Domitran, "Influence of profile shift on the spur gear pair optimization," *Mechanism and Machine Theory*, vol. 117, pp. 189–197, 2017.
- [15] Genetic algorithm and direct search toolbox 2, User's Guide.
- [16] G. Stanley and R. Bart, "Optimal population size and the genetic algorithm," 2000.
- [17] A. E. Smith and D. W. Coit, "Penalty functions," in *Handbook of Evolutionary Computation* Institute of Physics Publishing and Oxford University Press, Bristol, UK, 1997.
- [18] R. P. Durbin, A. BAchir, E. M. Boudi, and I. Amarir, "The effect of Addendum factor on contact ratio factor and contact stress for spur gears," in *Proceedings of the 2019 7th International Renewable and Sustainable Energy Conference (IRSEC)*, p. 1726, Agadir, Morocco, November 2019.
- [19] R. MAITI and A. K. ROY, "Minimum tooth difference in internal-external involute gear pair," *Mechanism and Machine Theory*, vol. 31, no. 4, pp. 475–485, 1996.
- [20] J. Colbourne, *The Geometry of Involute Gears*, Springer, Berlin, Germany, 1987.
- [21] M. G. Mariam, *Effect of change of contact ratio on contact fatigue michael gmariam these.*, Ph.D. thesis, Addis Ababa, Ethiopia, February 2013.
- [22] J. Shigley, *Mechanical Engineering Design*, McGraw-Hill, New York City, NY, USA, Eighth edition, 2006.
- [23] B.-R. Höhn, "Improvements on noise reduction and efficiency of gears," *Meccanica*, vol. 45, no. 3, pp. 425–437, 2010.
- [24] International Organization for Standardization, *ISO Standard 6336-1: 2006 Part 1: Basic Principles, Introduction and General Influence Factors*, International Organization for Standardization, Geneva, Switzerland, 2006.
- [25] K. Michaelis, B.-R. Höhn, and M. Hinterstoifser, "Influence factors on gearbox power loss," *Industrial Lubrication and Tribology*, vol. 63, no. 1, pp. 46–55, 2011.
- [26] A. R. Hassan, "Contact stress analysis of spur gear teeth pair," *Engineering and Technology*, vol. 3, no. 10, 2009.
- [27] X. Deng, L. Hua, and X. Han, "Research on the design and modification of asymmetric spur gear," *Mathematical Problems in Engineering*, vol. 201513 pages, 2015.
- [28] G. Niemann and M. Winter, *Band 2*, Springer, New York City, NY, USA, 2003.
- [29] C. Naruse, S. Haizuka, R. Nemoto, and K. Kurokawa, "Studies on frictional loss, temperature rise and limiting load for scoring of spur gear," *Bulletin of JSME*, vol. 29, no. 248, pp. 600–608, 1986.
- [30] T. Petry-Johnson, A. Kahraman, N. Anderson, and D. Chase, "An experimental investigation of spur gear efficiency," *Journal of Mechanical Design*, vol. 130, no. 6, 2008.